Frequency-Response Masking Approach for the Synthesis of Sharp Two-Dimensional Diamond-Shaped Filters

Yong Ching Lim and Seo How Low

***Abstract*— The frequency-response masking (FRM) technique is an efficient method for realizing sharp one-dimensional (1-D) filters. Sharp 1-D filters realized using the FRM technique have considerably lower complexity than those realized in the direct form. In this paper, we present an extension of the FRM technique to the synthesis of sharp two-dimensional (2-D) diamond-shaped (DS) filters. The new technique, based upon dividing the frequency spectrum into four complementary components and the utilization of four masking filters, achieves large reductions in filter implementation complexity when the transition width of the desired DS filter is very narrow. An expression for the impulse response up-sampling ratio that produces the design with the least complexity is derived. Extensions of the technique for the synthesis of 2-D filters other than the DS filters are also discussed.**

I. Introduction

LINEAR phase finite impulse response (FIR) digital filters are frequently used in signal processing applications for their guaranteed stability and freedom from phase distortion. One disadvantage of FIR filters is their high implementation complexities. This is especially so for sharp filters since the filter transition width is inversely proportional to the filter length [1]. Thus, the implementation of a sharp filter would entail an extremely long filter length and considerable arithmetic complexity. One technique that alleviates this problem is to implement the filter using the frequency-response masking (FRM) approach [2].

The FRM technique uses the fact that up-sampling the impulse response of a filter by inserting zeros reduces its transition width by the up-sampling ratio. For example, if each delay element of a prototype low-pass FIR filter $F_a(\omega)$ (subsequently called the band-edge shaping filter) is replaced by M delay elements, another FIR filter $F'_a(\omega)$, which has a transition width that is $1/M$ times that of the filter $F_a(\omega)$, is formed. The complement of the filter $F'_a(\omega)$, denoted by $F'_c(\omega)$, can be easily obtained by subtracting the output of the filter $F'_a(\omega)$ from a suitably delayed version of the input. By properly masking the frequency responses of the filters $F'_a(\omega)$ and $F'_c(\omega)$ and then recombining them, narrow transition-band filters can be obtained [2].

Further developments of the FRM technique have been reported in the literature. For example, [3] and [4] extend the method to the design of bandpass filters. Several authors, notably [5] and [6], sought to reduce the implementation complexity further by combining the frequency-response masking approach with the interpolated impulse response technique [7] or using half-band filters to serve as one of the masking filters. Applications of the FRM method in the implementation of linear phase filter banks are demonstrated in [8] and [9] while the optimum design of filters using the FRM technique is considered in [10]. Subsequent developments are also reported in [11]–[14]. Despite all these developments, the FRM technique has not been applied very successfully to the synthesis of two-dimensional (2-D) filters.

The high complexity problem of implementing sharp FIR filters is even more acute for 2-D filters. For the 2-D diamond-shaped (DS) filter, empirical results indicate that the filter support size is inversely proportional to the square of the transition width [15]–[17]. Thus, the complexity of a sharp DS filter would be prohibitively high. To implement sharp 2-D filters, new efficient techniques are needed. In [10], a method for the design of sharp 2-D filters using the FRM technique was described; however, the technique presented can only design filters with narrow passbands. In this paper, we present a design methodology that overcomes this limitation. We extend the FRM technique to the synthesis of sharp 2-D DS filters. The synthesis procedure is very similar to the one-dimensional (1-D) FRM counterpart; the difference is in the way the complementary components are selected. In our technique, instead of utilizing two complementary components and two masking filters, four complementary components and four masking filters are used. By combining the outputs obtained from passing the complementary components through carefully selected masking filters, sharp DS filters can be synthesized. This approach gives efficient realizations of sharp DS filters with arbitrary bandwidths and is not limited to narrow passband cases.

This paper is organized as follows. In Section II, we give a formal definition of the 2-D filters used in this paper, while in Section III, we demonstrate the design of DS filters with narrow passbands. This design methodology has limited practical usage. The FRM approach for the synthesis of DS filters is presented in Section IV. This section presents the design procedure as well as the definitions of the band edges of the band-edge shaping and masking filters. In Section V, we conduct an investigation of the relationship between the ripple performance of the synthesized filter and that of the

Manuscript received February 4, 1997; revised January 6, 1998. This paper was recommended by Associate Editor N. K. Bose.

The authors are with the Department of Electrical Engineering, National University of Singapore, Singapore 119260.

Publisher Item Identifier S 1057-7130(98)08504-8.

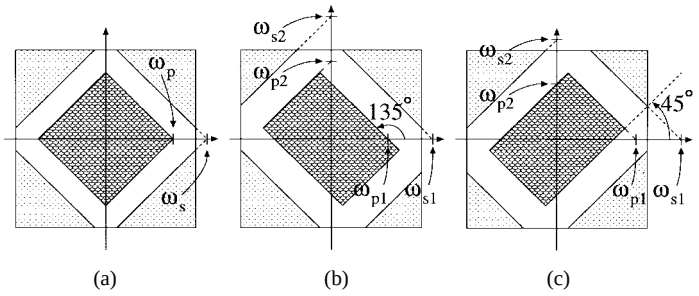

Fig. 1. Band-edge specifications of the DS, RS1, and RS2 filters.

band-edge shaping and masking filters. This provides valuable insight for the filter designer on how to optimize the ripple performance of the synthesized filter. Details on how to select the impulse response up-sampling ratio that produces the design with the minimum complexity is presented in Section VI. Finally, a design example and a brief discussion of the possible extensions of the 2-D FRM technique are presented in Section VII.

II. Definitions and Notations

The parameters that define the 2-D filters used in the FRM technique are as follows. The passband- and stopband-edges of the DS low-pass filter are denoted by ω_p and ω_s, respectively; ω_p and ω_s are the frequency values where the respective band edges (extrapolated if necessary) meet the frequency axes [see Fig. 1(a)]. The transition width of the DS filter is given by

$$\Delta_{ds} = \frac{\omega_s - \omega_p}{2\pi}. \tag{1}$$

We define two rectangular-shaped (RS) 2-D low-pass filters which are used as masking filters. The first RS filter, denoted by RS1, has the longer side of the rectangular passband at an angle of 135° to the horizontal frequency axis as illustrated in Fig. 1(b). The second RS filter, denoted by RS2, is shown in Fig. 1(c). It has the longer side of the rectangular passband at an angle of 45° to the horizontal frequency axis. For both the RS1 and RS2 filters, the passband and stopband edges are defined by $\omega_{p1}, \omega_{p2}, \omega_{s1}$, and ω_{s2}, respectively. ω_{p1} and ω_{s1} define the band edges which are at an angle of 135° to the horizontal frequency axis; these are, respectively, the frequency values where the passband- and stopband-edges meet the horizontal frequency axis. The band-edges which are at an angle of 45° to the horizontal frequency axis are defined by ω_{p2} and ω_{s2}. These are the frequency values where the passband and stopband edges meet the vertical frequency axis. The transition width of the RS filter is given by

$$\boldsymbol{\Delta}_{rs} = \frac{\boldsymbol{\Omega}_s - \boldsymbol{\Omega}_p}{2\pi} \tag{2}$$

where

$$\boldsymbol{\Omega}_p = [\omega_{p1} \quad \omega_{p2}]^T \tag{3a}$$

$$\boldsymbol{\Omega}_s = [\omega_{s1} \quad \omega_{s2}]^T. \tag{3b}$$

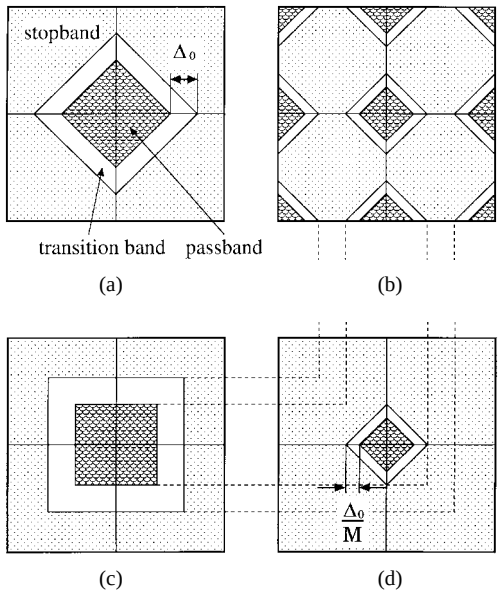

Fig. 2. Design of a DS filter with narrow passband.

III. Narrow Passband Filter Design

In this section, we consider how DS filters with narrow passbands may be designed. The procedure is similar to the narrow-band 2-D filter design technique presented in [10]. Consider the DS filter $F(\boldsymbol{\Omega})$ where $\boldsymbol{\Omega} = (\omega_1, \omega_2)$, shown in Fig. 2(a). If the impulse response of the filter is up-sampled by a factor of M ($M = 2$ in the example) in the vertical and horizontal dimensions by inserting zeros, the frequency response of the filter $F'(\boldsymbol{\Omega})$ shown in Fig. 2(b) is obtained. The up-sampling process introduces "images" of the DS passband into the 2-D region $[-\pi, \pi]^2$. A low complexity square-shaped filter [shown in Fig. 2(c)], easily derived by cascading two 1-D filters, can be used as a masking filter to remove these "images" to give the filter with the frequency response shown in Fig. 2(d).

It is evident that this technique produces a DS filter with a transition width that is $1/M$ times the original transition width. However, the bandwidth of the filter is also reduced by the same factor. Indeed, to obtain a filter with a very narrow transition width, the bandwidth of the filter would be very narrow. Such a design technique is therefore useful only for some specific applications and is not suitable for synthesizing wide-band filters. Our proposed design methodology overcomes this limitation.

IV. Arbitrary Bandwidth Design

The FRM filter design technique hinges on how the frequency spectrum is divided into suitable complementary components. For the case of 1-D filters, this can be done by splitting the frequency spectrum into two components [2]. There is no known simple rule that extends this two-complementary-component procedure to synthesize arbitrary-shaped 2-D filter. However, in this paper, we show that by dividing the frequency spectrum into four suitably chosen complementary components and using appropriate masking filters, the FRM technique can be applied to the design of DS filters.

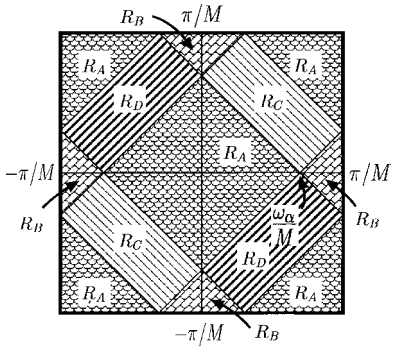

Fig. 3. The four frequency regions for the complementary components.

A. Complementary Components

The complementary components are defined by four 2-D frequency regions, R_A, R_B, R_C, and R_D. In the 2-D region $[-\pi/M, \pi/M]^2$, where M is the impulse response up-sampling ratio, these are shown in Fig. 3 and defined as follows:

$$R_A = \left\{ \boldsymbol{\Omega} \,\middle|\, \left| |\omega_1| + |\omega_2| - \frac{\pi}{M} \right| > \frac{\omega_\gamma}{M}, \; |\omega_1| \le \frac{\pi}{M}, |\omega_2| \le \frac{\pi}{M} \right\} \tag{4a}$$

$$R_B = \left\{ \boldsymbol{\Omega} \,\middle|\, |\omega_1 + \omega_2| > \frac{\omega_\alpha}{M}, |\omega_1 - \omega_2| > \frac{\omega_\alpha}{M}, \; |\omega_1| \le \frac{\pi}{M}, |\omega_2| \le \frac{\pi}{M} \right\} \tag{4b}$$

$$R_C = \left\{ \boldsymbol{\Omega} \,\middle|\, |\omega_1 + \omega_2| > \frac{\omega_\alpha}{M}, |\omega_1 + \omega_2| < \frac{\pi + \omega_\gamma}{M}, \; |\omega_1 - \omega_2| < \frac{\omega_\alpha}{M} \right\} \tag{4c}$$

$$R_D = \left\{ \boldsymbol{\Omega} \,\middle|\, |\omega_1 - \omega_2| > \frac{\omega_\alpha}{M}, |\omega_1 - \omega_2| < \frac{\pi + \omega_\gamma}{M}, \; |\omega_1 + \omega_2| < \frac{\omega_\alpha}{M} \right\}. \tag{4d}$$

In (4), ω_α/M is the frequency value at the intersection of the four regions (see Fig. 3) and $\omega_\gamma = \pi - \omega_\alpha$.

Note that while the definitions above are explicitly for the 2-D region $[-\pi/M, \pi/M]^2$, it should be interpreted in such a way that these regions are also defined for the periodic repetitions of the 2-D region $[-\pi/M, \pi/M]^2$. For example, $\boldsymbol{\Omega}_i \in R_A$ would imply that $\boldsymbol{\Omega}_i + (2\pi/M)\boldsymbol{\kappa} \in R_A$, where $\boldsymbol{\kappa}$ is the set of all two-component integers.

From Fig. 3, it can be observed that each component forms an "island" and is surrounded by the other complementary components. For example, component A is surrounded by components B, C, and D. Four complementary components are used because, geometrically, it is not possible to synthesize a DS filter by using three or fewer components. The separation between two "islands" of the same type is the allowance for the transition band of the masking filter for that component.

Let the prototype band-edge shaping filter $F_{\hat{Y}}(\boldsymbol{\Omega})$, where $Y \in \{A, B, C, D\}$, have the ideal frequency response such that if $M = 1$ in Fig. 3, the gain is unity in region R_Y and zero elsewhere. Component Y is then obtained by passing the input through the filter $F_{\hat{Y}}(\boldsymbol{\Omega})$. In general, $M \neq 1$ and component Y is obtained by applying $F'_{\hat{Y}}(\boldsymbol{\Omega})$ to the input instead, where $F'_{\hat{Y}}(\boldsymbol{\Omega})$ is the filter obtained by up-sampling by M times the impulse response of $F_{\hat{Y}}(\boldsymbol{\Omega})$ with zeros in both the horizontal and vertical dimensions.

B. Implementation

In the FRM technique for the design of 1-D filters, it is a trivial matter to obtain the two complementary components since the complement of one component can be easily obtained by subtracting the filtered output from a suitably delayed version of the input. However, this is not the case when four complementary components are required. One way to overcome this problem is to design the four band-edge shaping filters and introduce an "error" filter $F'_\varepsilon(\boldsymbol{\Omega})$ associated with an "error" component $\varepsilon(\boldsymbol{\Omega})$ to enforce the complementary criterion.

The block diagram of the technique is illustrated in Fig. 4. In Fig. 4, $X(\boldsymbol{\Omega})$ is the input and $F'_{\hat{A}}(\boldsymbol{\Omega}), F'_{\hat{B}}(\boldsymbol{\Omega}), F'_{\hat{C}}(\boldsymbol{\Omega})$, and $F'_{\hat{D}}(\boldsymbol{\Omega})$ are the 2-D band-edge shaping filters with the desired frequency responses as described previously. The components $A(\boldsymbol{\Omega}), B(\boldsymbol{\Omega}), C(\boldsymbol{\Omega})$, and $D(\boldsymbol{\Omega})$ are given by

$$\begin{aligned} A(\boldsymbol{\Omega}) &= F'_{\hat{A}}(\boldsymbol{\Omega})X(\boldsymbol{\Omega}) + \varepsilon(\boldsymbol{\Omega})/4 \\ B(\boldsymbol{\Omega}) &= F'_{\hat{B}}(\boldsymbol{\Omega})X(\boldsymbol{\Omega}) + \varepsilon(\boldsymbol{\Omega})/4 \\ C(\boldsymbol{\Omega}) &= F'_{\hat{C}}(\boldsymbol{\Omega})X(\boldsymbol{\Omega}) + \varepsilon(\boldsymbol{\Omega})/4 \\ D(\boldsymbol{\Omega}) &= F'_{\hat{D}}(\boldsymbol{\Omega})X(\boldsymbol{\Omega}) + \varepsilon(\boldsymbol{\Omega})/4 \end{aligned} \tag{5}$$

and the "error" component $\varepsilon(\boldsymbol{\Omega})$ is given by

$$\varepsilon(\boldsymbol{\Omega}) = F'_\varepsilon(\boldsymbol{\Omega})X(\boldsymbol{\Omega}) \tag{6}$$

where

$$F'_\varepsilon(\boldsymbol{\Omega}) = 1 - F'_{\hat{A}}(\boldsymbol{\Omega}) - F'_{\hat{B}}(\boldsymbol{\Omega}) - F'_{\hat{C}}(\boldsymbol{\Omega}) - F'_{\hat{D}}(\boldsymbol{\Omega}). \tag{7}$$

We shall use the notation $F'_Y(\boldsymbol{\Omega})$ to denote the transfer function from $X(\boldsymbol{\Omega})$ to component $Y(\boldsymbol{\Omega})$, i.e.,

$$Y(\boldsymbol{\Omega}) = F'_Y(\boldsymbol{\Omega})X(\boldsymbol{\Omega}) \tag{8a}$$

where $F'_Y(\boldsymbol{\Omega})$ is given by

$$F'_Y(\boldsymbol{\Omega}) = F'_{\hat{Y}}(\boldsymbol{\Omega}) + \frac{1}{4} F'_\varepsilon(\boldsymbol{\Omega}). \tag{8b}$$

If $F'_\varepsilon(\boldsymbol{\Omega}) = 0 \; \forall \, \Omega$, then $F'_{\hat{A}}(\boldsymbol{\Omega}), F'_{\hat{B}}(\boldsymbol{\Omega}), F'_{\hat{C}}(\boldsymbol{\Omega})$, and $F'_{\hat{D}}(\boldsymbol{\Omega})$ form a set of complementary filters. For practical band-edge shaping filters, $F'_\varepsilon(\boldsymbol{\Omega})$ is nonzero and $F'_{\hat{A}}(\boldsymbol{\Omega}), F'_{\hat{B}}(\boldsymbol{\Omega}), F'_{\hat{C}}(\boldsymbol{\Omega})$, and $F'_{\hat{D}}(\boldsymbol{\Omega})$ do not form a complementary set. However, with the introduction of $F'_\varepsilon(\boldsymbol{\Omega}), F'_A(\boldsymbol{\Omega}), F'_B(\boldsymbol{\Omega}), F'_C(\boldsymbol{\Omega})$, and $F'_D(\boldsymbol{\Omega})$ do form a complementary set, i.e.,

$$F'_A(\boldsymbol{\Omega}) + F'_B(\boldsymbol{\Omega}) + F'_C(\boldsymbol{\Omega}) + F'_D(\boldsymbol{\Omega}) = 1. \tag{9}$$

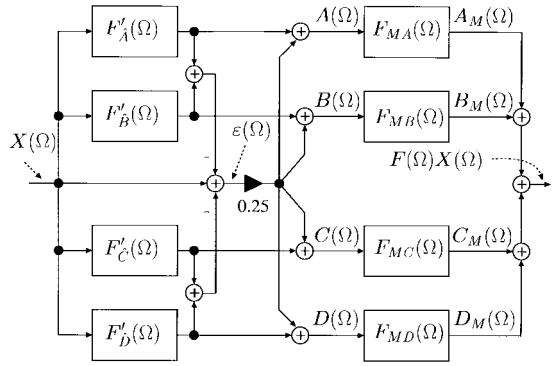

Fig. 4. Block diagram illustrating the frequency-response masking technique.

Note the distinction between $F'_Y(\boldsymbol{\Omega})$ and $F'_{\hat{Y}}(\boldsymbol{\Omega})$; the relationship between them is defined in (8b).

In the subsequent step, each of the components $A(\boldsymbol{\Omega}), B(\boldsymbol{\Omega}), C(\boldsymbol{\Omega})$, and $D(\boldsymbol{\Omega})$ is passed through the respective masking filter $(F_{MA}(\boldsymbol{\Omega}), F_{MB}(\boldsymbol{\Omega}), F_{MC}(\boldsymbol{\Omega})$, or $F_{MD}(\boldsymbol{\Omega}))$ to obtain $A_M(\boldsymbol{\Omega}), B_M(\boldsymbol{\Omega}), C_M(\boldsymbol{\Omega})$, and $D_M(\boldsymbol{\Omega})$. The final output $F(\boldsymbol{\Omega})X(\boldsymbol{\Omega})$ is obtained by summing $A_M(\boldsymbol{\Omega}), B_M(\boldsymbol{\Omega}), C_M(\boldsymbol{\Omega})$, and $D_M(\boldsymbol{\Omega})$. Obviously, appropriate delay elements, which are not shown in Fig. 4, must be added in an actual implementation.

The band-edge shaping and masking filters may be designed using the linear programming filter design technique. This technique is well reported in the literature [18]–[20]. It involves the optimization of the frequency response of the filter to satisfy a given set of specifications on a dense grid of frequency points. The masking filters may be designed by the direct application of this technique. However, for the band-edge shaping filters, the design procedure should be modified. The reason is as follows. If the four band-edge shaping filters are designed independently, there is no guarantee that $\varepsilon(\boldsymbol{\Omega})$ will be small in the transition area between any two regions. This poses a potential problem since if $\varepsilon(\boldsymbol{\Omega})$ is large, the ripple magnitude of the overall synthesized filter can be severely degraded. Thus, instead of designing the four band-edge shaping filters independently, they should be jointly optimized. The set of design constraints should be as follows:

$$-\delta_u \le F'_{\hat{Y}}(\Omega_s) \le \delta_u \tag{10a}$$

$$1-\delta_u \le F'_{\hat{Y}}(\Omega_p) \le 1+\delta_u \tag{10b}$$

$$\begin{aligned} 1-\rho\,\delta_u \le{}& F'_{\hat{A}}(\Omega_t)+F'_{\hat{B}}(\Omega_t)+F'_{\hat{C}}(\Omega_t) \\ &+F'_{\hat{D}}(\Omega_t) \\ \le{}& 1+\rho\,\delta_u \end{aligned} \tag{10c}$$

for $Y \in \{A,B,C,D\}$ and where δ_u is the ripple variable, Ω_s and Ω_p are, respectively, in the stopband and passband of $F'_Y(\boldsymbol{\Omega})$ and Ω_t is in the transition band of any of the filters $\{F'_{\hat{A}}(\boldsymbol{\Omega}), F'_{\hat{B}}(\boldsymbol{\Omega}), F'_{\hat{C}}(\boldsymbol{\Omega}), F'_{\hat{D}}(\boldsymbol{\Omega})\}$. The quantity ρ in (10c) controls the "tightness" of the bounds on the summation of $F'_{\hat{A}}(\boldsymbol{\Omega}), F'_{\hat{B}}(\boldsymbol{\Omega}), F'_{\hat{C}}(\boldsymbol{\Omega}), F'_{\hat{D}}(\boldsymbol{\Omega})$. As will be evident later in Sections V and VI, ρ should be selected such that $\rho \ll 1$.

We shall illustrate the FRM technique for the case where M is three. The frequency responses of $F'_A(\boldsymbol{\Omega})$, $F'_B(\boldsymbol{\Omega}), F'_C(\boldsymbol{\Omega})$, and $F'_D(\boldsymbol{\Omega})$ are shown in Fig. 5(a)–(d). Four masking filters, $F_{MA}(\boldsymbol{\Omega}), F_{MB}(\boldsymbol{\Omega}), F_{MC}(\boldsymbol{\Omega})$, and $F_{MD}(\boldsymbol{\Omega})$, with the frequency responses as shown superimposed onto the complementary filters in Fig. 5(a)–(d), are cascaded to the filters $F'_A(\boldsymbol{\Omega}), F'_B(\boldsymbol{\Omega}), F'_C(\boldsymbol{\Omega})$, and $F'_D(\boldsymbol{\Omega})$, respectively. By summing the outputs from the masking filters, the frequency response $F(\boldsymbol{\Omega})$ of the resulting filter, shown in Fig. 5(e), is obtained. Notice that the corners of the filter $F(\boldsymbol{\Omega})$ are contributed from the passband of the filter $F'_A(\boldsymbol{\Omega})$. We shall refer to this as CASE A.

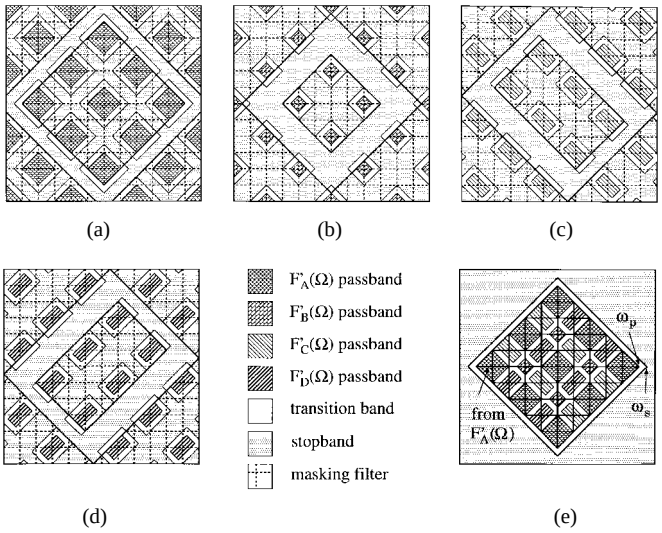

Fig. 5. Frequency response masks for CASE A.

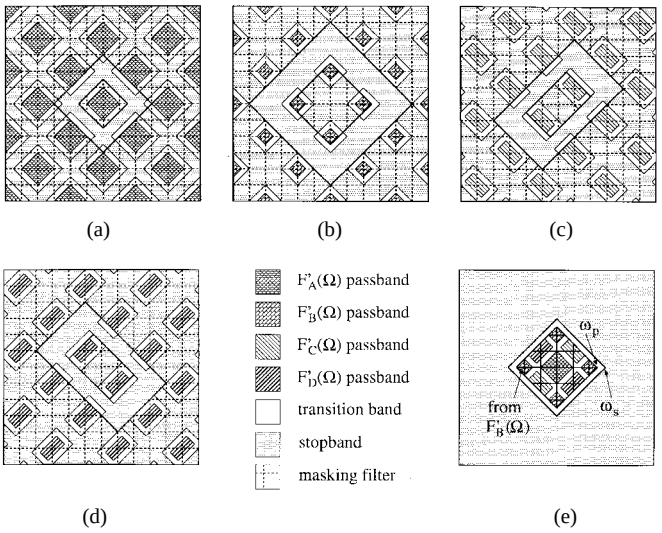

Fig. 6. Frequency response masks for CASE B.

On the other hand, if the masking filters have the frequency responses as shown in Fig. 6(a)–(d), then the resulting filter response is that shown in Fig. 6(e). In such a case, the corners of the passband of $F(\boldsymbol{\Omega})$ are contributed by the passband of $F'_B(\boldsymbol{\Omega})$ and shall be designated as CASE B.

C. Band-Edge Shaping and Masking Filters Specifications

We shall now derive the specifications of the band-edge shaping and masking filters given the specifications of the final desired DS filter. Suppose the band edges of the desired filter

$F(\boldsymbol{\Omega})$ are ψ_p and ψ_s, i.e., $\omega_p = \psi_p, \omega_s = \psi_s$, and the transition width is $\Delta_{ds} = (\psi_s - \psi_p/2\pi)$. Also, let the transition width of the band-edge shaping filters in the horizontal (or vertical) frequency dimension be Δ_α (all the transition widths of the band-edge shaping filters being equal) and define

$$\theta = \omega_\alpha - \pi\Delta_\alpha, \qquad \phi = \omega_\alpha + \pi\Delta_\alpha. \tag{11}$$

It can be shown that ψ_p and ψ_s are related to θ and ϕ by

$$\psi_p = \frac{2m\pi + \theta}{M} \tag{12a}$$

$$\psi_s = \frac{2m\pi + \phi}{M} \tag{12b}$$

where $0 \le m \le M-1$ for CASE A, and

$$\psi_p = \frac{2m\pi - \phi}{M} \tag{13a}$$

$$\psi_s = \frac{2m\pi - \theta}{M} \tag{13b}$$

where $1 \le m \le M$ for CASE B, m being an integer.

In a synthesis problem, ψ_p and ψ_s are known and m, M, θ, ϕ, ω_α, Δ_α, and the band edges of the masking filters must be determined. We shall express m, θ, and ϕ in terms of ψ_p, ψ_s, and M. Since

$$0 < \theta < \phi < \pi \tag{14}$$

to ensure that (12) yields a solution for CASE A, we have

$$m = \lfloor \psi_p M/(2\pi) \rfloor \tag{15a}$$

$$\theta = \psi_p M - 2m\pi \tag{15b}$$

$$\phi = \psi_s M - 2m\pi \tag{15c}$$

where $\lfloor x \rfloor$ denotes the largest integer less than x. For CASE B, we have

$$m = \lceil \psi_s M/(2\pi) \rceil \tag{16a}$$

$$\theta = 2m\pi - \psi_s M \tag{16b}$$

$$\phi = 2m\pi - \psi_p M \tag{16c}$$

where $\lceil x \rceil$ denotes the smallest integer larger than x. For any given set of ω_p, ω_s, and M, at most one of CASE A [(12) and (15)] or CASE B [(13) and (16)] will yield a set of θ and ϕ that satisfies (14). Irrespective of CASE A or CASE B, Δ_{ds} is given by

$$\Delta_{ds} = \frac{\psi_s - \psi_p}{2\pi} = \frac{\Delta_\alpha}{M}. \tag{17}$$

The transition width of the band-edge shaping filters is therefore M times the transition width of the synthesized filter. The value of ω_α may be obtained from (11) by substituting for the values of Δ_α, θ, and ϕ.

Note that it is also possible that for a given value of M, neither CASE A nor CASE B is valid. Such a situation occurs when the transition band of the filter to be synthesized does not lie completely between two adjacent folding frequency axes. The folding frequency axes are the diagonal lines (at both 45° and 135° to the horizontal axis) passing through

$$\omega_{fd} = \left\{ \omega | \omega = \frac{\pi\kappa}{M} \right\} \tag{18}$$

TABLE I
SPECIFICATIONS OF THE MASKING FILTERS FOR CASE A

Filter	Type	ω_p, $\boldsymbol{\Omega}_p$	ω_s, $\boldsymbol{\Omega}_s$
$F_{MA}(\boldsymbol{\Omega})$	DS	$\frac{2m\pi+\theta}{M}$	$\frac{2(m+1)\pi-\phi}{M}$
$F_{MB}(\boldsymbol{\Omega})$	DS	$\frac{2m\pi-\theta}{M}$	$\frac{2m\pi+\phi}{M}$
$F_{MC}(\boldsymbol{\Omega})$	RS1	$\frac{2m\pi-\theta}{M}$ $\frac{2m\pi+\theta}{M}$	$\frac{2m\pi+\phi}{M}$ $\frac{2(m+1)\pi-\phi}{M}$
$F_{MD}(\boldsymbol{\Omega})$	RS2	$\frac{2m\pi+\theta}{M}$ $\frac{2m\pi-\theta}{M}$	$\frac{2(m+1)\pi-\phi}{M}$ $\frac{2m\pi+\phi}{M}$

TABLE II
SPECIFICATIONS OF THE MASKING FILTERS FOR CASE B

Filter	Type	ω_p, $\boldsymbol{\Omega}_p$	ω_s, $\boldsymbol{\Omega}_s$
$F_{MA}(\boldsymbol{\Omega})$	DS	$\frac{2(m-1)\pi+\phi}{M}$	$\frac{2m\pi-\theta}{M}$
$F_{MB}(\boldsymbol{\Omega})$	DS	$\frac{2m\pi-\phi}{M}$	$\frac{2m\pi+\theta}{M}$
$F_{MC}(\boldsymbol{\Omega})$	RS2	$\frac{2m\pi-\phi}{M}$ $\frac{2(m-1)\pi+\phi}{M}$	$\frac{2m\pi+\theta}{M}$ $\frac{2m\pi-\theta}{M}$
$F_{MD}(\boldsymbol{\Omega})$	RS1	$\frac{2(m-1)\pi+\phi}{M}$ $\frac{2m\pi-\phi}{M}$	$\frac{2m\pi-\theta}{M}$ $\frac{2m\pi+\theta}{M}$

where κ is an integer. In such a case, another value of M must be selected. The value of M selected must satisfy the conditions $\psi_p > (\pi k/M)$ and $\psi_s < (\pi(k+1)/M)$, i.e.,

$$\frac{\pi k}{\psi_p} < M < \frac{\pi(k+1)}{\psi_s} \tag{19}$$

where $k = \lfloor \psi_p M/\pi \rfloor$. This condition ensures that the transition band of the synthesized filter lies completely between two adjacent folding frequencies. For example, it is not possible to synthesize a filter with $\psi_p = 0.6\pi, \psi_s = 0.7\pi$ for $M = 3$ since $(\pi k/\psi_p) = 1.667$ and $(\pi(k+1)/\psi_s) = 2.857$ in (19).

The specifications of the masking filters $F_{MA}(\boldsymbol{\Omega})$, $F_{MB}(\boldsymbol{\Omega}), F_{MC}(\boldsymbol{\Omega})$, and $F_{MD}(\boldsymbol{\Omega})$ depend on whether $F(\boldsymbol{\Omega})$ belongs to CASE A or CASE B. For CASE A, $F_{MA}(\boldsymbol{\Omega})$ and $F_{MB}(\boldsymbol{\Omega})$ are diamond-shaped filters and $F_{MC}(\boldsymbol{\Omega})$ and $F_{MD}(\boldsymbol{\Omega})$ are RS1 and RS2 filters, respectively. The band-edge specifications are given in Table I. For CASE B, the specifications are given in Table II. As in the 1-D case, "don't care" bands may be introduced when designing the masking filters to reduce complexity.

Up to this point, nothing has been said about how the value of M should be selected [other than the conditions listed in (19)]. One selection criterion is to choose the value of M that results in a design with the minimum number of multipliers. This shall be discussed in Section VI. Before we proceed to that, we must first examine the effects of the ripple magnitudes of the band-edge shaping filters and masking filters on the overall ripple magnitude of $F(\boldsymbol{\Omega})$.

V. RIPPLES OF $F(\boldsymbol{\Omega})$

In the discussion that follows, let $G_Y(\boldsymbol{\Omega})$ denote the desired gain of the filter $F_Y(\boldsymbol{\Omega})$, i.e., $G_Y(\boldsymbol{\Omega})$ has a value of unity in the passband and zero in the stopband. The ripple or deviation of $F_Y(\boldsymbol{\Omega})$ from $G_Y(\boldsymbol{\Omega})$ is defined as

$$\delta_Y(\boldsymbol{\Omega}) = F_Y(\boldsymbol{\Omega}) - G_Y(\boldsymbol{\Omega}). \tag{20}$$

For convenience, we shall assume that for the filters $F'_A(\boldsymbol{\Omega}), F'_B(\boldsymbol{\Omega}), F'_C(\boldsymbol{\Omega})$, and $F'_D(\boldsymbol{\Omega})$

$$G'_A(\boldsymbol{\Omega}) = F'_A(\boldsymbol{\Omega}), \quad G'_B(\boldsymbol{\Omega}) = F'_B(\boldsymbol{\Omega})$$
$$G'_C(\boldsymbol{\Omega}) = F'_C(\boldsymbol{\Omega}), \quad G'_D(\boldsymbol{\Omega}) = F'_D(\boldsymbol{\Omega}) \tag{21}$$

in their respective transition bands, i.e., the ripple magnitudes are zero in the transition bands. To simplify the analysis, we will only consider the first-order terms and neglect the higher order terms.

A. Ripples $\delta'_A(\boldsymbol{\Omega}), \delta'_B(\boldsymbol{\Omega}), \delta'_C(\boldsymbol{\Omega})$, and $\delta'_D(\boldsymbol{\Omega})$

We shall first obtain expressions for the ripples of the complementary filters $F'_A(\boldsymbol{\Omega}), F'_B(\boldsymbol{\Omega}), F'_C(\boldsymbol{\Omega})$, and $F'_D(\boldsymbol{\Omega})$. Note that we do not consider the transition bands since the ripple magnitudes are defined to be zero, i.e., for the filter $F'_Y(\boldsymbol{\Omega})$, we neglect the region that falls into the transition band of $F'_Y(\boldsymbol{\Omega})$.

From (8b), $F'_A(\boldsymbol{\Omega})$ is given by

$$F'_A(\boldsymbol{\Omega}) = \frac{1}{4}\left[1 - F'_{\hat{B}}(\boldsymbol{\Omega}) - F'_{\hat{C}}(\boldsymbol{\Omega}) - F'_{\hat{D}}(\boldsymbol{\Omega}) + 3F'_{\hat{A}}(\boldsymbol{\Omega})\right]. \tag{22}$$

Using (20), we can write (22) as

$$G'_A(\boldsymbol{\Omega}) + \delta'_A(\boldsymbol{\Omega}) \cdot \left[1 - G'_{\hat{B}}(\boldsymbol{\Omega}) - \delta'_{\hat{B}}(\boldsymbol{\Omega}) - G'_{\hat{C}}(\boldsymbol{\Omega}) - \delta'_{\hat{C}}(\boldsymbol{\Omega}) - G'_{\hat{D}}(\boldsymbol{\Omega}) - \delta'_{\hat{D}}(\boldsymbol{\Omega}) + 3G'_{\hat{A}}(\boldsymbol{\Omega}) + 3\delta'_{\hat{A}}(\boldsymbol{\Omega})\right]. \tag{23}$$

For the band-edge shaping filters, we have

$$G'_{\hat{A}}(\boldsymbol{\Omega}) + G'_{\hat{B}}(\boldsymbol{\Omega}) + G'_{\hat{C}}(\boldsymbol{\Omega}) + G'_{\hat{D}}(\boldsymbol{\Omega}) = 1 \quad \forall\, \Omega. \tag{24}$$

Therefore, (23) becomes

$$G'_A(\boldsymbol{\Omega}) + \delta'_A(\boldsymbol{\Omega}) = G'_{\hat{A}}(\boldsymbol{\Omega}) + \frac{1}{4}\left[3\delta'_{\hat{A}}(\boldsymbol{\Omega}) - \delta'_{\hat{B}}(\boldsymbol{\Omega}) - \delta'_{\hat{C}}(\boldsymbol{\Omega}) - \delta'_{\hat{D}}(\boldsymbol{\Omega})\right]. \tag{25}$$

For regions not in the transition band of $F'_A(\boldsymbol{\Omega})$, $G'_A(\boldsymbol{\Omega}) = G'_{\hat{A}}(\boldsymbol{\Omega})$. So we have

$$\delta'_A(\boldsymbol{\Omega}) = \frac{1}{4}\left[3\delta'_{\hat{A}}(\boldsymbol{\Omega}) - \delta'_{\hat{B}}(\boldsymbol{\Omega}) - \delta'_{\hat{C}}(\boldsymbol{\Omega}) - \delta'_{\hat{D}}(\boldsymbol{\Omega})\right]. \tag{26a}$$

For the ripples $\delta'_B(\boldsymbol{\Omega}), \delta'_C(\boldsymbol{\Omega})$, and $\delta'_D(\boldsymbol{\Omega})$, it can be easily shown using a similar procedure that the following results hold:

$$\delta'_B(\boldsymbol{\Omega}) = \tfrac{1}{4}\left[-\delta'_{\hat{A}}(\boldsymbol{\Omega}) + 3\delta'_{\hat{B}}(\boldsymbol{\Omega}) - \delta'_{\hat{C}}(\boldsymbol{\Omega}) - \delta'_{\hat{D}}(\boldsymbol{\Omega})\right] \tag{26b}$$
$$\delta'_C(\boldsymbol{\Omega}) = \tfrac{1}{4}\left[-\delta'_{\hat{A}}(\boldsymbol{\Omega}) - \delta'_{\hat{B}}(\boldsymbol{\Omega}) + 3\delta'_{\hat{C}}(\boldsymbol{\Omega}) - \delta'_{\hat{D}}(\boldsymbol{\Omega})\right] \tag{26c}$$
$$\delta'_D(\boldsymbol{\Omega}) = \tfrac{1}{4}\left[-\delta'_{\hat{A}}(\boldsymbol{\Omega}) - \delta'_{\hat{B}}(\boldsymbol{\Omega}) - \delta'_{\hat{C}}(\boldsymbol{\Omega}) + 3\delta'_{\hat{D}}(\boldsymbol{\Omega})\right]. \tag{26d}$$

B. Ripples of the Synthesized Filter

Using the notations defined earlier, we can write

$$\begin{aligned} G(\boldsymbol{\Omega}) + \delta(\boldsymbol{\Omega}) &= [G_{MA}(\boldsymbol{\Omega}) + \delta_{MA}(\boldsymbol{\Omega})][G'_A(\boldsymbol{\Omega}) + \delta'_A(\boldsymbol{\Omega})] \\ &\quad + [G_{MB}(\boldsymbol{\Omega}) + \delta_{MB}(\boldsymbol{\Omega})][G'_B(\boldsymbol{\Omega}) + \delta'_B(\boldsymbol{\Omega})] \\ &\quad + [G_{MC}(\boldsymbol{\Omega}) + \delta_{MC}(\boldsymbol{\Omega})][G'_C(\boldsymbol{\Omega}) + \delta'_C(\boldsymbol{\Omega})] \\ &\quad + [G_{MD}(\boldsymbol{\Omega}) + \delta_{MD}(\boldsymbol{\Omega})][G'_D(\boldsymbol{\Omega}) + \delta'_D(\boldsymbol{\Omega})] \end{aligned} \tag{27}$$

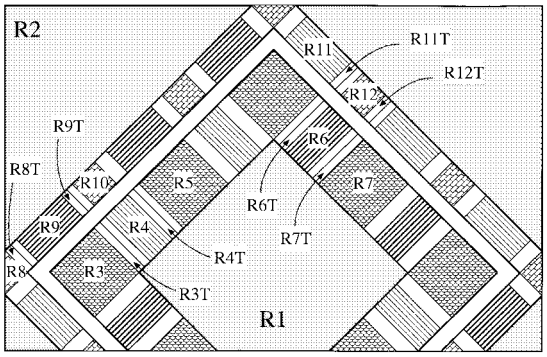

Fig. 7. Definition of the frequency regions for ripple magnitude analysis for CASE A.

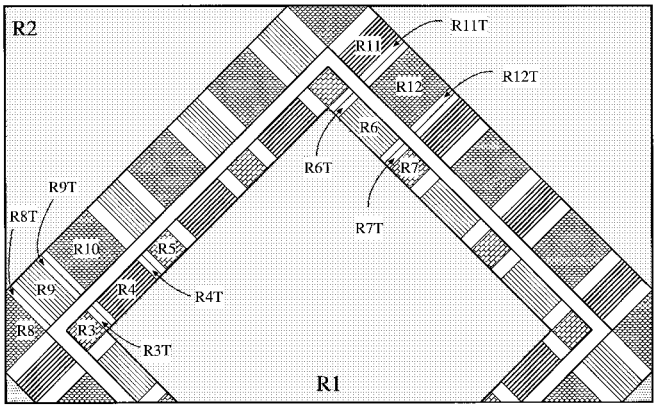

Fig. 8. Definition of the frequency regions for ripple magnitude analysis for CASE B.

where $G(\boldsymbol{\Omega})$ and $\delta(\boldsymbol{\Omega})$ are, respectively, the desired value and the deviation of the synthesized filter $F(\boldsymbol{\Omega})$. To analyze the ripple magnitude of the synthesized filter, we shall divide the 2-D region $[-\pi, \pi]^2$ into several regions.

The first region R_1 is the region where the desired values of the four masking filters are unity, i.e., $G_{MA}(\boldsymbol{\Omega}) = G_{MB}(\boldsymbol{\Omega}) = G_{MC}(\boldsymbol{\Omega}) = G_{MD}(\boldsymbol{\Omega}) = 1$, $\Omega \in R_1$. This region is illustrated in Fig. 7 for CASE A and Fig. 8 for CASE B. Substituting these values and $G(\boldsymbol{\Omega}) = 1$ into (27) and using the fact that $F'_A(\boldsymbol{\Omega}), F'_B(\boldsymbol{\Omega}), F'_C(\boldsymbol{\Omega})$, and $F'_D(\boldsymbol{\Omega})$ are complementary filters, we have

$$\begin{aligned} \delta(\boldsymbol{\Omega}) &= \delta_{MA}(\boldsymbol{\Omega})G'_A(\boldsymbol{\Omega}) + \delta_{MB}(\boldsymbol{\Omega})G'_B(\boldsymbol{\Omega}) \\ &\quad + \delta_{MC}(\boldsymbol{\Omega})G'_C(\boldsymbol{\Omega}) + \delta_{MD}(\boldsymbol{\Omega})G'_D(\boldsymbol{\Omega}). \end{aligned} \tag{28}$$

Using (24), we obtain

$$|\delta(\boldsymbol{\Omega})| \le \max\{|\delta_{MA}(\boldsymbol{\Omega})|, |\delta_{MB}(\boldsymbol{\Omega})|, |\delta_{MC}(\boldsymbol{\Omega})|, |\delta_{MD}(\boldsymbol{\Omega})|\}. \tag{29}$$

The second region, R_2, is defined to be the region where the desired gains of the four masking filters are zero, i.e., $G_{MA}(\boldsymbol{\Omega}) = G_{MB}(\boldsymbol{\Omega}) = G_{MC}(\boldsymbol{\Omega}) = G_{MD}(\boldsymbol{\Omega}) = 0$, $\Omega \in R_2$ (as illustrated in Fig. 7 for CASE A and Fig. 8 for CASE B). Substituting these values together with $G(\boldsymbol{\Omega}) = 0$ into (27), we obtain (28). As in region R_1, it can be shown that $\delta(\boldsymbol{\Omega})$ is also given by (29).

TABLE III
DESIRED FILTER GAINS IN EACH FREQUENCY REGION FOR CASE A

	$\Omega \in$	G	G_{MA}	G_{MB}	G_{MC}	G_{MD}	G'_A	G'_B	G'_C	G'_D	Remarks
R_3	R_A	1	1	T	T	T	1	0	0	0	
R_4	R_C	1	1	T	1	T	0	0	1	0	
R_5	R_A	1	1	T	1	T	1	0	0	0	
R_6	R_D	1	1	T	T	1	0	0	0	1	
R_7	R_A	1	1	T	T	1	1	0	0	0	
R_{3T}	R_A	1	1	T	1	T	T	0	T	0	$\delta'_A = \delta'_C = 0$
R_{4T}	R_C	1	1	T	1	T	T	0	T	0	$\delta'_A = \delta'_C = 0$
R_{6T}	R_D	1	1	T	T	1	T	0	0	T	$\delta'_A = \delta'_D = 0$
R_{7T}	R_A	1	1	T	T	1	T	0	0	T	$\delta'_A = \delta'_D = 0$
R_8	R_B	0	T	0	0	0	0	1	0	0	
R_9	R_D	0	T	0	T	0	0	0	0	1	
R_{10}	R_B	0	T	0	T	0	0	1	0	0	
R_{11}	R_C	0	T	0	0	T	0	0	1	0	
R_{12}	R_B	0	T	0	0	T	0	1	0	0	
R_{8T}	R_B	0	T	0	T	0	0	T	0	T	$\delta'_B = \delta'_D = 0$
R_{9T}	R_D	0	T	0	T	0	0	T	0	T	$\delta'_B = \delta'_D = 0$
R_{11T}	R_C	0	T	0	0	T	0	T	T	0	$\delta'_B = \delta'_C = 0$
R_{12T}	R_B	0	T	0	0	T	0	T	T	0	$\delta'_B = \delta'_C = 0$

Note: T = transition band; the desired gain ranges from zero to unity.

The above two regions cover the ripple magnitudes at frequencies not near to the transition band of the synthesized filter. To obtain the ripple magnitudes near the transition band of the synthesized filter, CASE A and CASE B must be analyzed separately. For CASE A, the regions (R_3 through R_{12T}) are defined as shown in Fig. 7 and the desired values of $F(\boldsymbol{\Omega})$, $F_{MA}(\boldsymbol{\Omega})$, $F_{MB}(\boldsymbol{\Omega})$, $F_{MC}(\boldsymbol{\Omega})$, $F_{MD}(\boldsymbol{\Omega})$, $F'_A(\boldsymbol{\Omega})$, $F'_B(\boldsymbol{\Omega})$, $F'_C(\boldsymbol{\Omega})$, and $F'_D(\boldsymbol{\Omega})$ in each of the region are tabulated in Table III. The values for the regions not explicitly defined in Fig. 7 may be obtained by symmetry.

From Table III, in region R_3, we have $G(\boldsymbol{\Omega}) = G'_A(\boldsymbol{\Omega}) = 1$ and $G'_B(\boldsymbol{\Omega}) = G'_C(\boldsymbol{\Omega}) = G'_D(\boldsymbol{\Omega}) = 0$; the frequency response of the masking filter $G_{MA}(\boldsymbol{\Omega})$ has unity gain while the other three masking filters, $G_{MB}(\boldsymbol{\Omega}), G_{MC}(\boldsymbol{\Omega})$ and $G_{MD}(\boldsymbol{\Omega})$, are in their transition bands. Substituting these values into (27), we obtain

$$\delta(\boldsymbol{\Omega}) = \delta_{MA}(\boldsymbol{\Omega}) + \delta'_A(\boldsymbol{\Omega}) + G_{MB}(\boldsymbol{\Omega})\delta'_B(\boldsymbol{\Omega}) + G_{MC}(\boldsymbol{\Omega})\delta'_C(\boldsymbol{\Omega}) + G_{MD}(\boldsymbol{\Omega})\delta'_D(\boldsymbol{\Omega})$$

which can be written as

$$\begin{aligned}\delta(\boldsymbol{\Omega}) = \delta_{MA}(\boldsymbol{\Omega}) &+ \frac{1}{4}\big[3 - G_{MB}(\boldsymbol{\Omega}) - G_{MC}(\boldsymbol{\Omega}) - G_{MD}(\boldsymbol{\Omega})\big]\delta'_{\hat{A}}(\boldsymbol{\Omega}) \\ &+ \frac{1}{4}\big[-1 + 3G_{MB}(\boldsymbol{\Omega}) - G_{MC}(\boldsymbol{\Omega}) - G_{MD}(\boldsymbol{\Omega})\big]\delta'_{\hat{B}}(\boldsymbol{\Omega}) \\ &+ \frac{1}{4}\big[-1 - G_{MB}(\boldsymbol{\Omega}) + 3G_{MC}(\boldsymbol{\Omega}) - G_{MD}(\boldsymbol{\Omega})\big]\delta'_{\hat{C}}(\boldsymbol{\Omega}) \\ &+ \frac{1}{4}\big[-1 - G_{MB}(\boldsymbol{\Omega}) - G_{MC}(\boldsymbol{\Omega}) + 3G_{MD}(\boldsymbol{\Omega})\big]\delta'_{\hat{D}}(\boldsymbol{\Omega}) \qquad (30)\end{aligned}$$

after substituting for $\delta'_A(\boldsymbol{\Omega}), \delta'_B(\boldsymbol{\Omega}), \delta'_C(\boldsymbol{\Omega})$, and $\delta'_D(\boldsymbol{\Omega})$ using (26a)–(26d). From (10), we have

$$\max\left\{|\delta'_{\hat{A}}(\boldsymbol{\Omega})|, |\delta'_{\hat{B}}(\boldsymbol{\Omega})|, |\delta'_{\hat{C}}(\boldsymbol{\Omega})|, |\delta'_{\hat{D}}(\boldsymbol{\Omega})|\right\} \le \delta_u \qquad (31)$$

in the passbands and stopbands. So we can write

$$|\delta(\boldsymbol{\Omega})| \le |\delta_{MA}(\boldsymbol{\Omega})| + J_{A3}(\boldsymbol{\Omega})\delta_u \qquad (32)$$

where $J_{A3}(\boldsymbol{\Omega})$ is given by

$$\begin{aligned}J_{A3}(\boldsymbol{\Omega}) = &\frac{1}{4}|3 - G_{MB}(\boldsymbol{\Omega}) - G_{MC}(\boldsymbol{\Omega}) - G_{MD}(\boldsymbol{\Omega})| \\ &+ \frac{1}{4}|-1 + 3G_{MB}(\boldsymbol{\Omega}) - G_{MC}(\boldsymbol{\Omega}) - G_{MD}(\boldsymbol{\Omega})| \\ &+ \frac{1}{4}|-1 - G_{MB}(\boldsymbol{\Omega}) + 3G_{MC}(\boldsymbol{\Omega}) - G_{MD}(\boldsymbol{\Omega})| \\ &+ \frac{1}{4}|-1 - G_{MB}(\boldsymbol{\Omega}) - G_{MC}(\boldsymbol{\Omega}) + 3G_{MD}(\boldsymbol{\Omega})|. \qquad (33)\end{aligned}$$

Given that $0 \le G_{MA}(\boldsymbol{\Omega}), G_{MB}(\boldsymbol{\Omega}), G_{MC}(\boldsymbol{\Omega}), G_{MD}(\boldsymbol{\Omega}) \le 1$ it can be shown that $0 \le J_{A3}(\boldsymbol{\Omega}) \le 2$. Thus, the expression for the ripple in R_3 is

$$|\delta(\boldsymbol{\Omega})| \le |\delta_{MA}(\boldsymbol{\Omega})| + 2\delta_u. \qquad (34)$$

Region R_{3T} is in the transition band of $F'_A(\boldsymbol{\Omega})$ and $F'_C(\boldsymbol{\Omega})$. Thus, $\delta'_A(\boldsymbol{\Omega}) = \delta'_C(\boldsymbol{\Omega}) = 0$. Also, $G_{MA}(\boldsymbol{\Omega}) = G_{MC}(\boldsymbol{\Omega}) = 1$ and $G'_B(\boldsymbol{\Omega}) = G'_D(\boldsymbol{\Omega}) = 0$. Substituting these values into (27) and using (26), we have

$$\begin{aligned}\delta(\boldsymbol{\Omega}) = &G'_A(\boldsymbol{\Omega})\delta_{MA}(\boldsymbol{\Omega}) + G'_C(\boldsymbol{\Omega})\delta_{MC}(\boldsymbol{\Omega}) \\ &+ G_{MB}(\boldsymbol{\Omega})\delta'_{\hat{B}}(\boldsymbol{\Omega}) \\ &+ G_{MD}(\boldsymbol{\Omega})\delta'_{\hat{D}}(\boldsymbol{\Omega}) + \frac{1}{4}[-G_{MB}(\boldsymbol{\Omega}) - G_{MD}(\boldsymbol{\Omega})] \\ &\cdot [\delta'_{\hat{A}}(\boldsymbol{\Omega}) + \delta'_{\hat{B}}(\boldsymbol{\Omega}) + \delta'_{\hat{C}}(\boldsymbol{\Omega}) + \delta'_{\hat{D}}(\boldsymbol{\Omega})]. \qquad (35)\end{aligned}$$

From (10c), (24), and (31), we obtain the following expression for the ripple in R_{3T}:

$$\begin{aligned}|\delta(\boldsymbol{\Omega})| &\le \max\{|\delta_{MA}(\boldsymbol{\Omega})|, |\delta_{MC}(\boldsymbol{\Omega})|\} \\ &\quad + [G_{MB}(\boldsymbol{\Omega}) + G_{MD}(\boldsymbol{\Omega})]\delta_u \\ &\quad + \frac{\rho\,\delta_u}{4}[G_{MB}(\boldsymbol{\Omega}) + G_{MD}(\boldsymbol{\Omega})] \\ &\le \max\{|\delta_{MA}(\boldsymbol{\Omega})|, |\delta_{MC}(\boldsymbol{\Omega})|\} + \left(2 + \frac{\rho}{2}\right)\delta_u. \qquad (36)\end{aligned}$$

Notice that for the δ_u term, there is an additional factor of $\rho/2$ in (36) when compared to (34). This additional factor can be made negligible by choosing $\rho \ll 1$.

The ripples in the regions R_4 through R_{12T} and that for CASE B may be obtained using a similar analysis. The appropriate values of $G(\boldsymbol{\Omega}), G'_A(\boldsymbol{\Omega}), G'_B(\boldsymbol{\Omega}), G'_C(\boldsymbol{\Omega}), G'_D(\boldsymbol{\Omega}), G_{MA}(\boldsymbol{\Omega}), G_{MB}(\boldsymbol{\Omega})$, $G_{MC}(\boldsymbol{\Omega})$, and $G_{MD}(\boldsymbol{\Omega})$ may be obtained from Table III for CASE A and Table IV for CASE B. The regions for CASE B are defined in Fig. 8. A summary of the results is as follows. Denoting the maximum ripple magnitudes in the passband and stopband of the synthesized filter by δ_p and δ_s, respectively, we have, for CASE A

$$\delta_p \le \max\{|\delta_{MA}(\boldsymbol{\Omega})|, |\delta_{MC}(\boldsymbol{\Omega})|, |\delta_{MD}(\boldsymbol{\Omega})|\} + \left(2 + \frac{\rho}{2}\right)\delta_u \qquad (37a)$$

$$\delta_s \le \max\{|\delta_{MB}(\boldsymbol{\Omega})|, |\delta_{MC}(\boldsymbol{\Omega})|, |\delta_{MD}(\boldsymbol{\Omega})|\} + \left(2 + \frac{\rho}{2}\right)\delta_u \qquad (37b)$$

TABLE IV
DESIRED FILTER GAINS IN EACH FREQUENCY REGION FOR CASE B

	$\Omega \in$	G	G_{MA}	G_{MB}	G_{MC}	G_{MD}	G'_A	G'_B	G'_C	G'_D	Remarks
R_3	R_B	1	T	1	T	T	0	1	0	0	
R_4	R_D	1	T	1	T	1	0	0	0	1	
R_5	R_B	1	T	1	T	1	0	1	0	0	
R_6	R_C	1	T	1	1	T	0	0	1	0	
R_7	R_B	1	T	1	1	T	0	1	0	0	
R_{3T}	R_B	1	T	1	T	1	0	T	0	T	$\delta'_B = \delta'_D = 0$
R_{4T}	R_D	1	T	1	T	1	0	T	0	T	$\delta'_B = \delta'_D = 0$
R_{6T}	R_C	1	T	1	1	T	0	T	T	0	$\delta'_B = \delta'_C = 0$
R_{7T}	R_B	1	T	1	1	T	0	T	T	0	$\delta'_B = \delta'_C = 0$
R_8	R_A	0	0	T	0	0	1	0	0	0	
R_9	R_C	0	0	T	0	T	0	0	1	0	
R_{10}	R_A	0	0	T	0	T	1	0	0	0	
R_{11}	R_D	0	0	T	T	0	0	0	0	1	
R_{12}	R_A	0	0	T	T	0	1	0	0	0	
R_{8T}	R_A	0	0	T	0	T	T	0	T	0	$\delta'_A = \delta'_C = 0$
R_{9T}	R_C	0	0	T	0	T	T	0	T	0	$\delta'_A = \delta'_C = 0$
R_{11T}	R_D	0	0	T	T	0	T	0	0	T	$\delta'_A = \delta'_D = 0$
R_{12T}	R_A	0	0	T	T	0	T	0	0	T	$\delta'_A = \delta'_D = 0$

Note: T = transition band; the desired gain ranges from zero to unity.

and for CASE B

$$\delta_p \le \max\{|\delta_{MB}(\boldsymbol{\Omega})|, |\delta_{MC}(\boldsymbol{\Omega})|, |\delta_{MD}(\boldsymbol{\Omega})|\} + \left(2 + \frac{\rho}{2}\right)\delta_u \tag{38a}$$

$$\delta_s \le \max\{|\delta_{MA}(\boldsymbol{\Omega})|, |\delta_{MC}(\boldsymbol{\Omega})|, |\delta_{MD}(\boldsymbol{\Omega})|\} + \left(2 + \frac{\rho}{2}\right)\delta_u. \tag{38b}$$

If the passband and stopband ripple magnitudes of the masking filters are equal, the results for CASE A and CASE B are identical.

VI. MINIMUM-COMPLEXITY DESIGN

In this section, we shall derive an expression for the value of M that minimizes the FRM implementation complexity. The number of multipliers required in an implementation will be used as a yardstick to measure the complexity of the technique. To facilitate the derivations for the minimum complexity design, the characteristics of the band-edge shaping and masking filters must be known. We shall use the results in [16], which state that for a rectangular-shaped filter with a support size of N by N, passband and stopband ripple magnitudes of δ_p and δ_s, respectively, and transition width $\boldsymbol{\Delta}_{rs} = [\Delta_1\ \Delta_2]^T$, the relationship between the variables can be approximated by

$$N \approx \frac{\Phi_2(\delta_p, \delta_s)}{\Delta_{\text{eqv}}} + 1 \tag{39a}$$

where

$$\Phi_2(\delta_p, \delta_s) = -0.299 - 0.568 \log_{10} \delta_p - 0.852 \log_{10} \delta_s \tag{39b}$$

and

$$\Delta_{\text{eqv}} = \min(\Delta_1, \Delta_2) + 0.07\sqrt{|\Delta_1 - \Delta_2|}. \tag{39c}$$

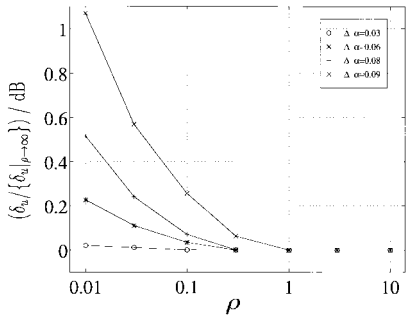

Fig. 9. $(\delta_u/\{\delta_u|_{\rho\to\infty}\})$ versus ρ plot for filters with $N = 17$ and $\omega_\alpha = 0.55\pi$.

For Δ_{eqv} small, the term $\Phi_2(\delta_p, \delta_s)/\Delta_{\text{eqv}}$ is dominant. We shall neglect the constant term and write

$$N \approx \frac{\Phi_2(\delta_p, \delta_s)}{\Delta_{\text{eqv}}}. \tag{40}$$

Consider a diamond-shaped filter $F(\boldsymbol{\Omega})$ with passband and stopband ripple magnitudes of not more than δ, transition width Δ_{ds}, and a support size of N_0 by N_0. Using (40), the number of multipliers P_0 required to implement this filter is given by

$$P_0 = N_0^2 \approx \left[\frac{\Phi_2(\delta, \delta)}{\Delta_{ds}}\right]^2. \tag{41}$$

Suppose that the FRM technique is used to synthesize this filter. Let the filter support sizes of the prototype band-edge shaping and masking filters be denoted using $N_Y \times N_Y$, where Y is the notation for the respective filter. To simplify the analysis, we shall assume that

$$\delta_{MM} = \max_{\Omega} \{|\delta_{MA}(\boldsymbol{\Omega})|, |\delta_{MB}(\boldsymbol{\Omega})|, |\delta_{MC}(\boldsymbol{\Omega})|, |\delta_{MD}(\boldsymbol{\Omega})|\} \tag{42}$$

in both the passbands and stopbands of the masking filters.

We now consider the number of multipliers required to implement the band-edge shaping filters. The formula for estimating the filter order was developed based upon the statistics of low-pass filters without imposing any transition band constraints. In the design of the band-edge shaping filters, the additional constraints in (10c) have been added. From our experience, the addition of the constraints does not significantly alter the value of the objective function (when compared to the case where the filters are designed independently). This is illustrated in Fig. 9 which shows the amount of alteration for different values of ρ and Δ_α for the set of filters with $N = 17$ and $\omega_\alpha = 0.55\pi$. The amount of alteration is computed by normalizing δ_u against $(\delta_u|_{\rho\to\infty})$, where $(\delta_u|_{\rho\to\infty})$ is the value of δ_u when the filters are designed independently (corresponding to $\rho \to \infty$). It can be observed from the graph that the deviation is larger for larger Δ_α. Nevertheless, for $\rho = 0.1$, the amount of alteration is not more than 0.3 dB ($\Delta_\alpha \le 0.09$). Since the majority of the band-edge shaping filters have $\Delta_\alpha \le 0.09$ and since the filter order is relatively insensitive to ripple magnitude, we can therefore use (39) to estimate the filter orders of the band-edge shaping filters.

The transition width of each band-edge shaping filter is M times the transition width of $F(\boldsymbol{\Omega})$, so we have

$$N_{\hat{A}} = N_{\hat{B}} = N_{\hat{C}} = N_{\hat{D}} \approx \frac{\Phi_2(\delta_u, \delta_u)}{M\Delta_{ds}}. \tag{43}$$

The impulse responses of the band-edge shaping filters have the characteristic that alternate coefficients are zero (see the Appendix). Thus, the number of multipliers required to implement the four band-edge shaping filters is given by

$$P_c = 4\left[\frac{N_{\hat{A}}^2}{2}\right] = 2N_{\hat{A}}^2 \approx 2\left[\frac{\Phi_2(\delta_u, \delta_u)}{M\Delta_{ds}}\right]^2. \tag{44}$$

Notice that the complexity required to implement the band-edge shaping filters is inversely proportional to M^2.

Let Δ_i and Δ_j be the transition widths of the filters $F_{MA}(\boldsymbol{\Omega})$ and $F_{MB}(\boldsymbol{\Omega})$, respectively. Then from Tables I and II, the transition widths of the filters $F_{MC}(\boldsymbol{\Omega})$ and $F_{MD}(\boldsymbol{\Omega})$ are given by $[\Delta_i\ \Delta_j]^T$ and $[\Delta_j\ \Delta_i]^T$ (the order may need to be interchanged depending on whether it is CASE A or CASE B; in any case, it does not affect our subsequent analysis) and that

$$\Delta_i + \Delta_j = \frac{1}{M}. \tag{45}$$

From (40), the number of multipliers required to implement the filters $F_{MA}(\boldsymbol{\Omega})$ and $F_{MB}(\boldsymbol{\Omega})$ are given by

$$N_{MA} \approx \frac{\Phi_2(\delta_{MM}, \delta_{MM})}{\Delta_i}$$

and

$$N_{MB} \approx \frac{\Phi_2(\delta_{MM}, \delta_{MM})}{\Delta_j},$$

respectively. The filters $F_{MC}(\boldsymbol{\Omega})$ and $F_{MD}(\boldsymbol{\Omega})$ are similar since one filter can be obtained from a 90°-rotation of the other. Without loss of generality, assume that $\Delta_j \geq \Delta_i$; in that case, N_{MC} (or N_{MD}) is given by

$$N_{MC} \approx \frac{\Phi_2(\delta_{MM}, \delta_{MM})}{\Delta_i + 0.07\sqrt{\Delta_j - \Delta_i}}. \tag{46}$$

The number of multipliers required to implement the four masking filters can therefore be approximated by

$$P_m \approx \left[\frac{\Phi_2(\delta_{MM}, \delta_{MM})}{\Delta_i}\right]^2 + \left[\frac{\Phi_2(\delta_{MM}, \delta_{MM})}{\Delta_j}\right]^2 + 2\left[\frac{\Phi_2(\delta_{MM}, \delta_{MM})}{\Delta_i + 0.07\sqrt{\Delta_j - \Delta_i}}\right]^2. \tag{47}$$

By substituting for Δ_i in (47) using (45), it can be shown that P_m attains its minimum value when

$$\Delta_i \approx \Delta_j \approx \frac{1}{2M}. \tag{48}$$

Substituting for Δ_i and Δ_j in (47) using (48) leads to

$$P_m = 4N_{MA}^2 \approx 16[M\Phi_2(\delta_{MM}, \delta_{MM})]^2. \tag{49}$$

It is clear from the above expression that the complexity required to implement the masking filters is directly proportional to M^2.

The total number of multipliers required in the FRM technique is thus given by

$$P_t = P_c + P_m \approx 2\left[\frac{\Phi_2(\delta_u, \delta_u)}{M\Delta_{ds}}\right]^2 + 16[M\Phi_2(\delta_{MM}, \delta_{MM})]^2. \tag{50}$$

When the value of M is increased, the complexity of the band-edge shaping filters decreases while that of the masking filters increases and vice versa. There is therefore an optimum value of M that minimizes the total complexity P_t. By differentiating P_t with respect to M and equating the derivative to zero, it can be shown that P_t is minimized when $P_c = P_m$. The value of M at minimum complexity, M_{opt}, is given by

$$M_{\text{opt}} \approx 8^{-(1/4)}\sqrt{\frac{\Phi_2(\delta_u, \delta_u)}{\Delta_{ds}\Phi_2(\delta_{MM}, \delta_{MM})}}. \tag{51}$$

The above expression provides valuable information on how the value of M can be selected.

If we further assume that $\delta_u \approx \delta_{MM}$, then M_{opt} is simply given by

$$M_{\text{opt}} \approx \frac{8^{-(1/4)}}{\sqrt{\Delta_{ds}}} \approx \frac{0.595}{\sqrt{\Delta_{ds}}} \tag{52}$$

and the number of multipliers at minimum complexity $P_{\min}$ is

$$P_{\min} = \frac{8\sqrt{2}[\Phi_2(\delta_u, \delta_u)]^2}{\Delta_{ds}}. \tag{53}$$

The total complexity is proportional to $1/\Delta_{ds}$, which is a significant improvement from proportional to $(1/\Delta_{ds})^2$ for the case of a direct-form implementation.

From (37) and (38) and choosing $\rho \ll 1$, we can write the ripple magnitude of the synthesized filter as

$$\delta \leq \delta_{MM} + 2\,\delta_u. \tag{54}$$

Writing

$$\delta_u \approx \delta/3 \tag{55}$$

we have

$$\Phi_2(\delta_u, \delta_u) \approx \Phi_2(\delta, \delta) + 0.678. \tag{56}$$

The FRM technique will produce a savings in the number of multipliers when compared to direct-form implementation provided that the transition width is smaller than a given limit. Thus, an important quantity is the transition width at the break-even point. This transition width Δ_b occurs when $P_{\min} = P_0$. Equating (41) and (53), we have

$$\Delta_b \approx \frac{\sqrt{2}}{16\zeta(\delta)} \approx \frac{0.088}{\zeta(\delta)} \tag{57}$$

where

$$\zeta(\delta) = \left[\frac{\Phi_2(\delta, \delta) + 0.678}{\Phi_2(\delta, \delta)}\right]^2. \tag{58}$$

The value of Δ_b depends on the ripple magnitude δ. From (58), it is clear that $\zeta(\delta) > 1$ and approaches unity when δ is small, i.e., an absolute bound for Δ_b is $\Delta_b < 0.088$. The behavior

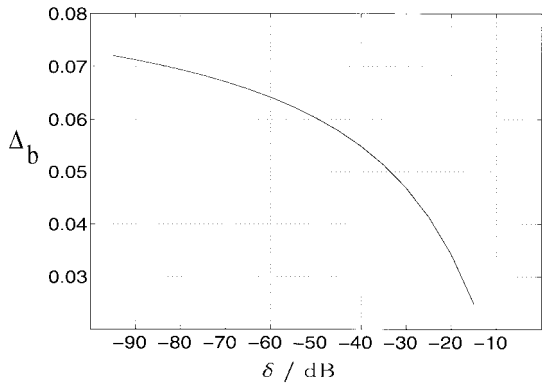

Fig. 10. Δ_b versus δ plot.

of Δ_b with respect to δ is illustrated in Fig. 10. For δ ranging from -80 dB to -20 dB, Δ_b ranges from 0.069–0.034.

In the derivations above, the minimum complexity is obtained when $\Delta_i \approx \Delta_j$. In practice, this condition may not be true as the band edges of the masking filters are determined by M and the band-edges of $F(\boldsymbol{\Omega})$. However, it is always possible to vary M in the vicinity of $M_{\rm opt}$ so that the condition holds. We shall therefore examine the sensitivity of P_t with respect to M in the vicinity of $M_{\rm opt}$.

Let the value of M in the vicinity of $M_{\rm opt}$ at which the condition $\Delta_i \approx \Delta_j$ holds be given by $M_{\rm opt}+\partial M$, where ∂M is small compared to $M_{\rm opt}$. Neglecting the higher powers of $\partial M/M_{\rm opt}$, it can be shown using (50) that

$$\frac{P_t|_{M=M_{\rm opt}+\partial M}}{P_t|_{M=M_{\rm opt}}} \approx 1+2\left[\frac{\partial M}{M_{\rm opt}}\right]^2-2\left[\frac{\partial M}{M_{\rm opt}}\right]^3. \quad (59)$$

P_t is thus not very sensitive to the value of M in the vicinity of $M_{\rm opt}$. For example, a 20% variation in the value of M about $M_{\rm opt}$ causes a variation of only 6% in the value of P_t.

VII. Design Example and Extensions

We shall illustrate the FRM technique by synthesizing a DS filter with $\omega_p = 0.5\pi, \omega_s = 0.52\pi$ and passband and stopband ripple magnitudes of not more than 0.12 (or -18.4 dB). From (52), we obtain $M = M_{\rm opt} = 5.95$. Checking with (12)–(16), we find that neither CASE A nor CASE B is valid. So we choose $M = 5$ instead, in which case the desired filter belongs to CASE A with $m = 1,\ \theta = 0.5\pi,\ \phi = 0.6\pi,\ \Delta_\alpha = 0.05$, and $\omega_\alpha = 0.55\pi$. Using these values, the band edges of the masking filters are obtained from Table I.

To ensure that the ripple magnitude of the synthesized filter satisfies the design requirements, from (54) and (55), we require the band-edge shaping and masking filters to each have passband and stopband ripple magnitudes of not more than -28.0 dB. The band-edge shaping filters that meet the above requirements have filter support sizes of 33 by 33 each and the masking filters have filter support sizes ranging from 17 by 17 to 21 by 21. In the design of the band-edge shaping filters, we have used $\rho = 0.1$.

Applying the FRM technique, the perspective and contour plots of the frequency magnitude response of the synthesized filter are shown in Fig. 11(a) and (b), respectively. Using

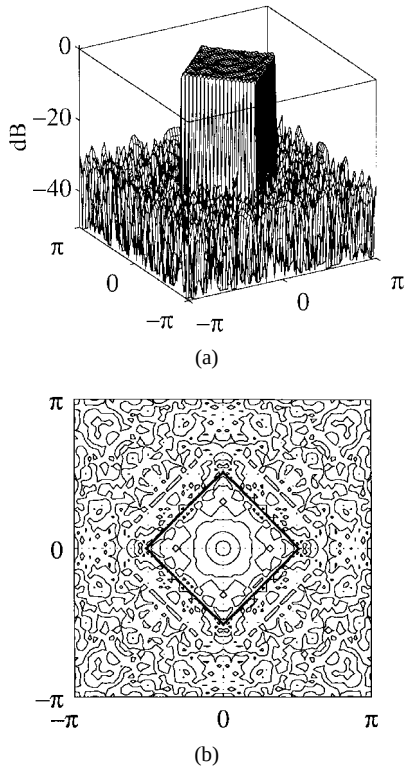

Fig. 11. The frequency response magnitude of the synthesized DS filter: (a) perspective plot and (b) contour plot.

a very dense grid[1] to check the frequency response of the synthesized filter, the maximum ripple magnitude was found to be -20.0 dB in the passband and -19.6 dB in the stopband. It therefore satisfies the design requirements.

To appreciate the amount of computational savings, we shall compare this design with a direct-form implementation. From the relationships presented in [15] and [16], a direct-form minimax DS filter with the same specifications would require a filter support size of at least 101 by 101. A rough estimate of the complexity reduction can be obtained by counting only the number of multipliers involved. In our implementation, there are approximately 2500 multiplications. This compares favorably with the 10 000 multiplications required in a direct-form implementation. There is therefore a savings in terms of the number of multipliers by a factor of four. For filters with sharper transition bands, higher orders of complexity reduction is possible. Note that the implementation complexity can be further reduced by applying the singular value decomposition technique [21]–[23] on the band-edge shaping and masking filters.

In this paper, we have introduced a new technique to synthesize sharp 2-D DS filters with an eight-fold symmetry. In fact, the FRM technique is general and can also be applied to implement 2-D filters with other frequency response regions of support as well as M-D filters. We illustrate in Fig. 12 some of the other 2-D filters that can be synthesized using the FRM technique. Fig. 12(a)–(b) illustrates how DS filters with four-fold symmetry may be implemented. The synthesis of

[1] 4096 by 4096 points in the frequency region $[-\pi, \pi]^2$.

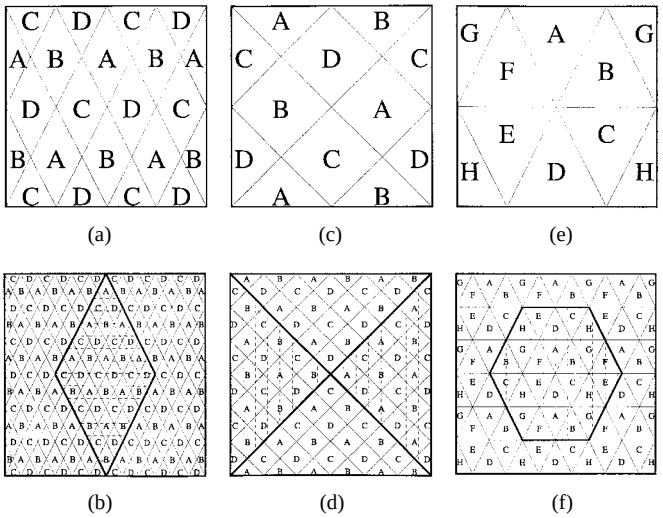

Fig. 12. Illustration of the synthesis of DS filters with (a), (b) four-fold symmetry, (c), (d) fan-shaped filters and (e), (f) hexagonal-shaped filters.

fan-shaped filters and hexagonal-shaped filters are illustrated in Fig. 12(c)–(d) and (e)–(f), respectively.

VIII. Conclusion

We have presented a new technique to implement sharp DS filters. This technique, which is an extension of the FRM approach for the synthesis of 1-D filters, produces filters with a considerably lower complexity when compared to direct-form implementations. The design procedure as well as the definitions of the band edges of the band-edge shaping and masking filters are presented in this paper. We have analyzed the relationship between the ripple magnitudes of the overall synthesized filter and that of the band-edge shaping and masking filters. An expression for the impulse response up-sampling ratio that produces the design with the minimum complexity is also derived. We have demonstrated the effectiveness of our design technique using a design example. Other 2-D filters that can be implemented using the FRM technique are also discussed.

Appendix

The frequency response of an FIR filter, with filter support size N by N (N odd) and impulse response $h(n_1, n_2)$, can be written as

$$H(\omega_1,\omega_2) = \sum_{n_1=-P}^{n_1=P} \sum_{n_2=-P}^{n_2=P} h(n_1,n_2) e^{-jn_1\omega_1} e^{-jn_2\omega_2} \tag{A-1}$$

where $P = (N-1)/2$. From the symmetry of the frequency response of the band-edge shaping filters, we have

$$H(\omega_1,\omega_2) = H(\pi-\omega_1,\pi-\omega_2) = H(-\omega_1,-\omega_2). \tag{A-2}$$

We can write $H(\pi-\omega_1,\pi-\omega_2)$ and $H(-\omega_1,-\omega_2)$ as

$$H(\pi-\omega_1,\pi-\omega_2) = -\left[\sum_{n_1=-P}^{n_1=P} \sum_{n_2=-P}^{n_2=P} h(n_1,n_2) e^{jn_1\omega_1} e^{jn_2\omega_2}\right]_{n_1+n_2=\text{odd}} + \left[\sum_{n_1=-P}^{n_1=P} \sum_{n_2=-P}^{n_2=P} h(n_1,n_2) e^{jn_1\omega_1} e^{jn_2\omega_2}\right]_{n_1+n_2=\text{even}} \tag{A-3}$$

and

$$H(-\omega_1,-\omega_2) = \left[\sum_{n_1=-P}^{n_1=P} \sum_{n_2=-P}^{n_2=P} h(n_1,n_2) e^{jn_1\omega_1} e^{jn_2\omega_2}\right]_{n_1+n_2=\text{odd}} + \left[\sum_{n_1=-P}^{n_1=P} \sum_{n_2=-P}^{n_2=P} h(n_1,n_2) e^{jn_1\omega_1} e^{jn_2\omega_2}\right]_{n_1+n_2=\text{even}} \tag{A-4}$$

respectively. Since (A-3) and (A-4) must be equal for all values of (ω_1,ω_2), it is clear that $h(n_1,n_2)=0$ when n_1+n_2 is odd, i.e., alternate coefficient values are zero.

References

[1] O. Herrmann, L. R. Rabiner, and D. S. K. Chan, "Practical design rules for optimum finite impulse response low-pass digital filters," *Bell Syst. Tech. J.*, vol. 52, no. 6, pp. 769–799, July–Aug. 1973.

[2] Y. C. Lim, "Frequency-response masking approach for the synthesis of sharp linear phase digital filters," *IEEE Trans. Circuits Syst.*, vol. 33, pp. 357–364, Apr. 1986.

[3] G. Rajan, Y. Neuvo, and S. K. Mitra, "On the design of sharp cutoff wide-band FIR filters with reduced arithmetic complexity," *IEEE Trans. Circuits Syst.*, vol. 35, pp. 1447–1454, Nov. 1988.

[4] ——, "Computationally efficient wide-band FIR filters with very narrow transition bands," in *Proc. IEEE Int. Symp. Circuits and Systems*, 1988, pp. 2013–2017.

[5] R. Yang, B. Liu, and Y. C. Lim, "A new structure of sharp transition FIR filters using frequency-response masking," *IEEE Trans. Circuits Syst.*, vol. 35, pp. 955–966, Aug. 1988.

[6] Y. Lian and Y. C. Lim, "Reducing the complexity of frequency response masking filters using half-band filters," *Signal Processing*, vol. 42, pp. 227–230, Mar. 1995.

[7] Y. Neuvo, C. Y. Dong, and S. K. Mitra, "Interpolated finite impulse response filters," *IEEE Trans. Acoust., Speech, Signal Processing*, vol. ASSP-32, pp. 563–570, June 1984.

[8] Y. C. Lim, "A digital filter bank for digital audio systems," *IEEE Trans. Circuits Syst.*, vol. 33, pp. 848–849, Aug. 1986.

[9] Y. Lian and Y. C. Lim, "Linear-phase digital audio tone control," *J. Audio Eng. Soc.*, vol. 35, pp. 38–40, Jan./Feb. 1987.

[10] Y. C. Lim and Y. Lian, "The optimum design of one- and two-dimensional FIR filters using the frequency response masking technique," *IEEE Trans. Circuits Syst. II*, vol. 40, pp. 88–95, Feb. 1993.

[11] ——, "Frequency-response masking approach for digital filter design: Complexity reduction via masking filter factorization," *IEEE Trans. Circuits Syst. II*, vol. 41, pp. 518–525, Aug. 1994.

[12] T. Saramäki, Y. C. Lim, and R. Yang, "The synthesis of half-band filter using frequency-response masking technique," *IEEE Trans. Circuits Syst. II*, vol. 42, pp. 58–60, Jan. 1995.

[13] C. K. Chen and J. H. Lee, "Design of sharp-cutoff FIR digital filters with prescribed constant group delay," *IEEE Trans. Circuits Syst. II*, vol. 43, pp. 1–13, Jan. 1996.

[14] M. G. Bellanger, "Improved design of long FIR filters using the frequency masking technique," in *Proc. IEEE Int. Conf. Acoustic, Speech, and Signal Processing*, vol. 3, 1996, pp. 1272–1275.

[15] P. Carrai, G. M. Cortelazzo, and G. A. Mian, "Characteristics of minimax FIR filters for video interpolation/decimation," *IEEE Trans. Circuits Syst. Video Technol.*, vol. 4, pp. 453–467, Oct. 1994.

[16] S. H. Low and Y. C. Lim, "Design rules for rectangular 2-D FIR low-pass filters," *Signal Processing*, vol. 54, pp. 99–102, Oct. 1996.

[17] Y. C. Lim and S. H. Low, "Practical design rules for minimax linear phase diamond-shaped 2-D FIR low-pass filters," *IEEE Trans. Circuits Syst. II*, vol. 44, pp. 966–970, Nov. 1997.

[18] J. V. Hu and L. R. Rabiner, "Design techniques for two-dimensional digital filters," *IEEE Trans. Audio, Electroacoust.*, vol. 20, pp. 249–257, Oct. 1972.

[19] Y. Kamp and J. P. Thiran, "Chebyshev approximation for two-dimensional nonrecursive digital filters," *IEEE Trans. Circuits Syst.*, vol. CS-22, pp. 208–218, Mar. 1975.
[20] Y. C. Lim, "Efficient special purpose linear programming for FIR filter design," *IEEE Trans. Acoustics, Speech, Signal Processing*, vol. ASSP-31, pp. 963–968, Aug. 1983.
[21] D. E. Dudgeon and R. M. Mersereau, *Multidimensional Digital Signal Processing*. Englewood Cliffs, NJ: Prentice-Hall, 1984.
[22] W. S. Lu and A. Antoniou, *Two-Dimensional Digital Filters*. New York: Marcel Dekker, 1992.
[23] W. S. Lu, H. P. Wang, and A. Antoniou, "Design of two-dimensional FIR digital filters by using the singular-value decomposition," *IEEE Trans. Circuits Syst.*, vol. 37, pp. 35–46, Jan. 1990.

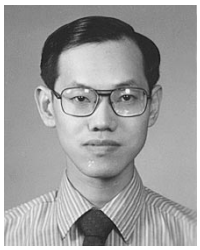

Yong Ching Lim received the A.C.G.I. and B.Sc. degrees in 1977 and the D.I.C and Ph.D. degrees in 1980, all in electrical engineering from Imperial College, the University of London, England.

From 1980 to 1982, he was a National Research Council Research Associate in the Naval Postgraduate School, Monterey, CA. He joined the Department of Electrical Engineering of the National University of Singapore in 1982. His research interests include VLSI circuits and systems design, digital signal processing, and design automation.

Dr. Lim served as an Associate Editor for the IEEE TRANSACTIONS ON CIRCUITS AND SYSTEMS from 1991 to 1993 and has been an Associate Editor for *Circuits, Systems and Signal Processing* since 1993. He was selected to receive the 1990 IREE (Australia) Norman Hayes Award and the 1996 IEEE Circuits and Systems Society's Guillemin Cauer Award.

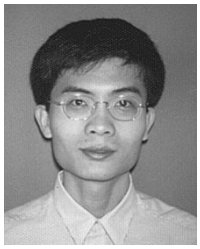

Seo How Low received the B.Eng. and Ph.D. degrees in electrical engineering from the National University of Singapore in 1994 and 1998, respectively.

Currently he is a postdoctoral fellow with the National University of Singapore. His research interests are in the areas of digital signal processing and VLSI circuits and systems design.